iScience

CellPress
OPEN ACCESS

Article

Loss of Polycystin-1 causes cAMP-dependent switch from tubule to cyst formation

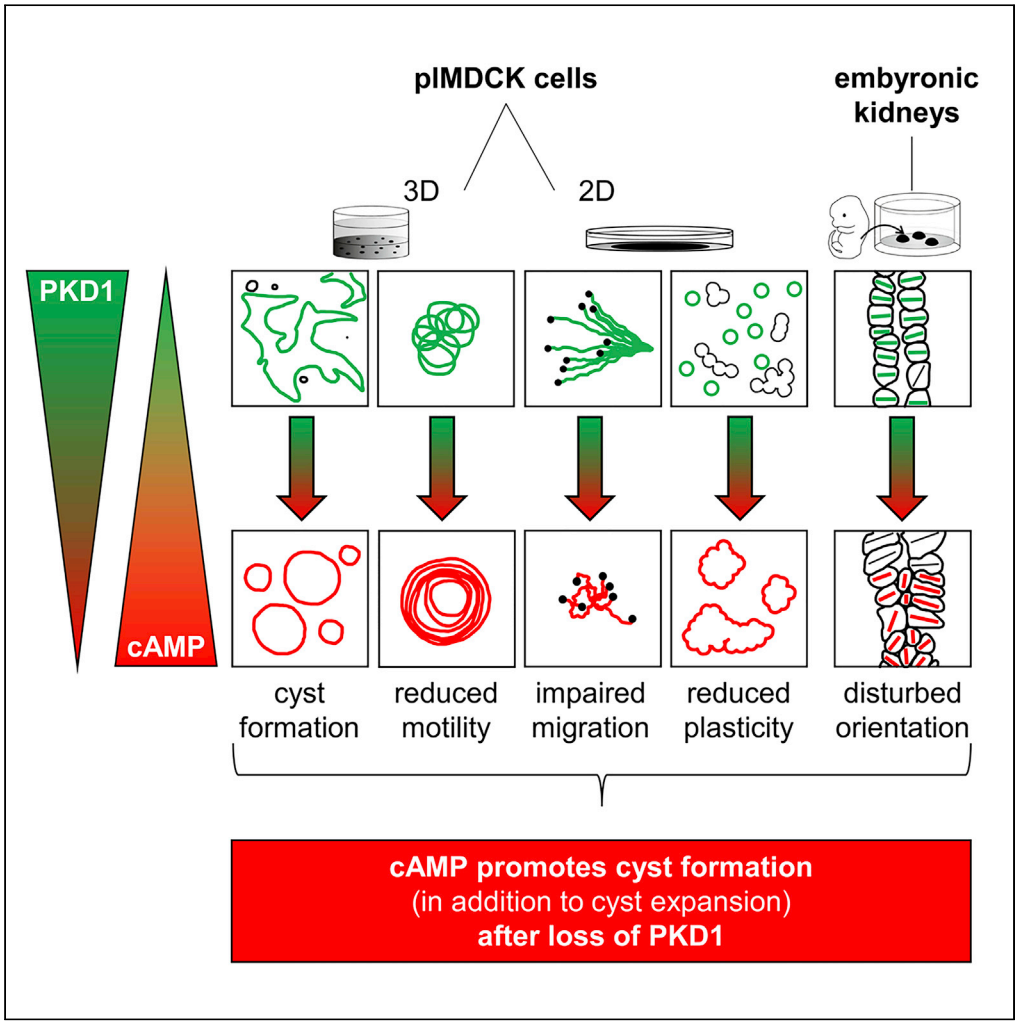

Julia Katharina Scholz, Andre Kraus, Dominik Lüder, ..., Steffen Grampp, Johannes Schödel, Bjoern Buchholz

bjoern.buchholz@uk-erlangen.de

Highlights

Loss of Polycystin-1 switches renal cells from tubule to cyst formation

Deletion of Polycystin-1 leads to increase in cAMP

Elevation of cAMP in wildtype cells phenocopies Polycystin-1-deficient features

Features are: impaired plasticity, nondirectional migration, and mis-orientation

Scholz et al., iScience 25, 104359
June 17, 2022
https://doi.org/10.1016/j.isci.2022.104359

iScience

CellPress
OPEN ACCESS

Article

Loss of Polycystin-1 causes cAMP-dependent switch from tubule to cyst formation

Julia Katharina Scholz,[1] Andre Kraus,[1] Dominik Lüder,[2] Kathrin Skoczynski,[1] Mario Schiffer,[1] Steffen Grampp,[1] Johannes Schödel,[1] and Bjoern Buchholz[1,3,*]

SUMMARY

Autosomal dominant polycystic kidney disease is the most common monogenic disease that causes end-stage renal failure. It primarily results from mutations in the PKD1 gene that encodes for Polycystin-1. How loss of Polycystin-1 translates into bilateral renal cyst development is mostly unknown. cAMP is significantly involved in cyst enlargement but its role in cyst initiation has remained elusive. Deletion of Polycystin-1 in collecting duct cells resulted in a switch from tubule to cyst formation and was accompanied by an increase in cAMP. Pharmacological elevation of cAMP in Polycystin-1-competent cells caused cyst formation, impaired plasticity, nondirectional migration, and mis-orientation, and thus strongly resembled the phenotype of Polycystin-1-deficient cells. Mis-orientation of developing tubule cells in metanephric kidneys upon loss of Polycystin-1 was phenocopied by pharmacological increase of cAMP in wildtype kidneys. *In vitro*, cAMP impaired tubule formation after capillary-induced injury which was further impaired by loss Polycystin-1.

INTRODUCTION

Autosomal dominant polycystic kidney disease (ADPKD) is the most common monogenic renal disease (Hildebrandt et al., 2011). ADPKD is characterized by the development of numerous bilateral cysts that enlarge continuously owing to increased cell proliferation and transepithelial fluid transport into the cysts' lumina (Chebib and Torres, 2016). Cyst enlargement leads to compression of adjacent nephrons which then results in a decline in kidney function (Grantham et al., 2011).

In most cases, ADPKD is caused by mutation of the PKD1 gene which encodes for Polycystin-1 (PC1) (Harris and Torres, 2009). Complete loss of PC1 is lethal, therefore, only one of the two alleles of the PKD1 gene reveals a germline mutation in ADPKD patients (Cornec-Le Gall et al., 2014). Cyst formation is thought to be initiated by an additional somatic mutation of the second allele (second hit) (Cornec-Le Gall et al., 2014). This results in a circumscribed dilation of the renal tubule leading to a sac-like structure, which eventually detaches from the tubule and forms a cyst (Grantham et al., 2011). The precise mechanisms leading to these tubular alterations are still elusive. However, in recent years, it has become evident that PC1-deficient cells exhibit an altered cell shape, changes in the actin cytoskeleton organization and impaired directed cell migration, which altogether is supposed to contribute to the tubular dilations following the second hit mutation (Nigro et al., 2015; Smith et al., 2020).

Existing therapy focuses on advanced stages of ADPKD, when cysts have already developed (Chebib et al., 2018). Numerous pathways have been found to mediate cyst enlargement (Chebib et al., 2015). Tolvaptan, the only existing targeted therapy for this disease, focuses on reduction of arginine vasopressin (AVP)-mediated increase in cAMP, which is known to be an important mediator of cyst growth by promoting apical chloride secretion and cyst cell proliferation (Torres et al., 2012). Next to AVP, increased activation of calcium-inhibitable adenylyl cyclases 5 and 6 as well as decreased cAMP hydrolysis due to inhibition of calcium-calmodulin-dependent phosphodiesterase type 1 (PDE1) may also contribute to cAMP upregulation in ADPKD (Gattone et al., 2003; Ye et al., 2016).

Although the role of cAMP for chloride secretion and cyst enlargement has been intensively studied, its potential involvement in the initiation of cyst formation has remained elusive so far. cAMP is the archetype of a second messenger and is involved in a plethora of signaling pathways affecting various cellular

[1]Department of Nephrology and Hypertension, Friedrich-Alexander-University Erlangen-Nuernberg, Ulmenweg 18, 91054 Erlangen, Germany

[2]Faculty of Computer Science, University of Applied Sciences, Augsburg, Germany

[3]Lead contact

*Correspondence: bjoern.buchholz@uk-erlangen.de

https://doi.org/10.1016/j.isci.2022.104359

characteristics (Sussman et al., 2020). Therefore, we wanted to test if alterations of cytosolic cAMP concentrations upon loss of PC1 may affect cell polarity and migration of renal tubule cells *in vitro* and *in vivo* and therefore contribute to the initiation of renal cyst formation. We therefore established a PC1-deficient cyst model. In ADPKD, cysts mainly originate from principal cells of the collecting duct (Raphael et al., 2009; Torres, 2004). Madin-Darby Canine Kidney (MDCK) cells are widely used to study physiological and pathophysiological properties of renal epithelial cells. They originate from the collecting duct, are highly polarized, and can be studied in three-dimensions within a collagen matrix (Buchholz et al., 2011). However, MDCK cells reveal the risk of clonal variability upon cell culture conditions and passaging of cells and often lack expression of detectable PC1 protein levels (Boca et al., 2007; Boletta et al., 2000). We therefore took advantage of our previously described and characterized plMDCK subclone (principal-like MDCK cells (Buchholz et al., 2014a), initially described as C7 clone (Gekle et al., 1994) which offers several advantages: i) it highly resembles principal cells which are the main origin of cyst formation in ADPKD, ii) due to its clonal character it is homogenous and keeps its properties over many passages, and iii) it expresses detectable endogenous protein levels of PC1.

Here, we analyzed the impact of PC1 deletion on cAMP levels of plMDCK cells and its effect on cell-cell organization, cell polarity, cell migration as well as cyst and tubule formation. In addition, alterations of renal tubule cells upon inducible tubule-specific loss of PC1 and increase of cAMP has been studied in embryonic kidneys.

RESULTS

PC1-competent plMDCK cells form tubular structures within a 3D matrix, whereas PC1-deficient cells form cysts spontaneously

In order to test for PC1-dependent effects in renal tubular cells, we generated clones of principal-like (pl) MDCK cells with a genetic deletion for PKD1 by the use of CRISPR/Cas9 technique. Figure S1 provides a detailed overview of the generation approach, sequencing data, and validation of knockout on protein level. plMDCK wild type as well as PC1-competent control clone cells (referred to as PKD1$^{+/+}$ in figures) form tubule-like structures within a collagen 1 matrix (Figures 1A, 1B, and S2). In contrast, two different clones of PC1-deficient cells (referred to as PKD1$^{-/-}$ #1 and PKD1$^{-/-}$ #2 in figures) mainly formed cysts spontaneously (Figures 1A and 1B). Since cAMP is an important promoter of cyst enlargement, we wanted to test its effect in our model. Interestingly, increase of cAMP in PKD1$^{+/+}$ and wild type cells by forskolin which activates the enzyme adenylyl cyclase and increases intracellular levels of cAMP resulted in a switch from tubule to cyst formation, mimicking the phenotype of PC1-deficient cells (Figures 1A, 1B, and S2). Of note, PC1-deficient cysts did not change their cystic phenotype in the presence of forskolin except for that cyst sizes were significantly increased compared to control condition and also compared to PKD1$^{+/+}$ cysts in the presence of forskolin (Figure 1B and S3). The increase of cyst size upon application of forskolin is in line with numerous previous findings that show that cAMP promotes secretion-dependent cyst enlargement (Terryn et al., 2011). In summary, PC1-deficiency and increase in cAMP led to cyst formation of plMDCK cells.

Loss of PC1 results in elevated levels of cAMP

Next, to evaluate cAMP as a driver of cyst initiation we tested for cAMP concentrations in PC1-competent (wild type and PKD1$^{+/+}$) cells and PC1-deficient cells (PKD1$^{-/-}$ #1 and PKD1$^{-/-}$ #2) (Figure 1C). cAMP levels were comparable in wild type and PKD1$^{+/+}$ cells. However, cAMP was significantly elevated in the PC1-deficient cell clones (Figure 1C). Forskolin significantly elevated cAMP concentrations in PC1-competent and PC1-deficient cells to a similar level (Figure 1C). These data suggested that the different levels of cAMP under control conditions may be causative for the phenotypic differences between PC1-deficient and PC1-competent cells within the 3D matrix.

PC1 deletion and increase of cAMP impair the motility of spheroids within a collagen matrix

In vitro tubulogenesis by MDCK cells undergoes a well-described 4-step process (Zegers et al., 2003). Cells first form small cystic aggregates followed by a few cells at the border sending out centrifugal extensions. The extensions then guide cells to migrate out of the aggregate and form a chain of cells. Cells then divide to form a cord and finally build a lumen by further separation. Extension formation and cell migration out of PC1-competent aggregates could be monitored by significant movements within the collagen matrix using live cell imaging (Figures 1D, 1E, and S4 and Video S1). In contrast, loss of PC1 resulted in significantly

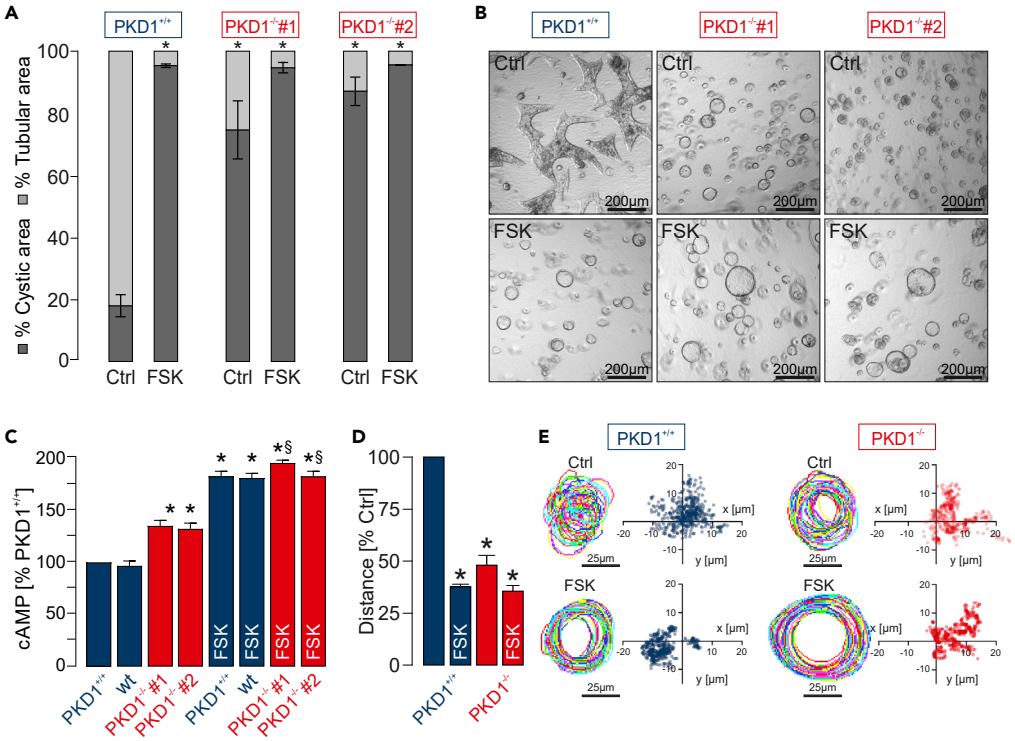

Figure 1. Deletion of PC1 results in a switch from tubulogenesis to cyst formation and is accompanied by an increase of cAMP and a decrease in cell motility

(A and B) PC1-competent clonal cells ($PKD1^{+/+}$) mainly formed tubule-like structures within a collagen matrix when incubated with control medium (Ctrl). In contrast, PC1-deficient cells ($PKD1^{-/-}$; shown for two different clones #1 and #2) primarily formed cysts within the collagen matrix in the presence of control medium (Ctrl). Application of forskolin (FSK; 10µM) to $PKD1^{+/+}$ cells turned them into cyst-forming cells resembling the phenotype obtained by PC1-deletion under control condition. Incubation of $PKD1^{-/-}$ cells with forskolin (FSK; 10µM) had no impact on their morphology.

(A) provides the analysis of the ratio of cystic to tubule-like formed structures (analysis of 128 images from n = 4 individual experiments).

(B) shows representative images after five days of culture within a collagen I matrix.

(C) Measurements of cAMP concentrations revealed similar values in clonal PC1-competent cells ($PKD1^{+/+}$) compared to wild type cells (wt). PC1-deletion resulted in significantly elevated cAMP levels in PC1-deficient cells ($PKD1^{-/-}$ #1 and #2) with $PKD1^{+/+}$ set as 100% (n = 6 individual experiments). Incubation of the cells with forskolin (FSK; 10µM) resulted in a significant increase of cAMP in PC1-competent and PC1-deficient cells to a similar level (n = 3 individual experiments).

(D and E) Movement of spheroids of PC1-competent and PC1-deficent cells (shown for $PKD1^{-/-}$ #1) within the collagen matrix was captured by live imaging of 30 spheroids per condition and cell type from n = 3 individual experiments for 48 h. Deletion of PC1 resulted in decreased motility. Incubation with forskolin (FSK; 10µM) also led to a reduction of motility in PC1-competent cells to a similar degree obtained from PC1-defcient cell under control condition. Application of forskolin to PC1-deficient spheroids had no additional effect. (D) Analysis of movements of spheroids within the matrix. (E) Representative traces of single spheroids within 48 h of imaging. *significant compared to $PKD1^{+/+}$-Ctrl; § significant compared to $PKD1^{-/-}$#1-FSK and $PKD1^{-/-}$#2-FSK, respectively. Data are represented as mean ± SEM. See also Figures S1–S5, and Video S1.

reduced movements (Figures 1D, 1E, and S4, and Video S1). Increase of cAMP by forskolin reduced the movement of PC1-competent aggregates to a similar degree as obtained from deletion of PC1 (Figures 1D, 1E, and S4, and Video S1). Incubation of PC1-deficient aggregates with forskolin did not further reduce movement (Figures 1D, 1E, and S4 and Video S1) suggesting a threshold of cAMP concentration that once exceeded turns the renal tubule cells from tubule-forming into a cyst-forming phenotype. In contrast, *in vitro* growth of PC1-deficient cysts could be further increased by raising cAMP concentrations with forskolin (Figure S3) which is in line with previous findings (Cabrita et al., 2020).

Next to cAMP, we have shown that hypoxia and subsequent activation of the hypoxia-inducible factor HIF-1α as well as ATP have significant impact on cyst enlargement by activation of calcium-activated chloride secretion (Buchholz et al., 2014b; Kraus et al., 2016a, 2018). Therefore, we analyzed whether inhibition

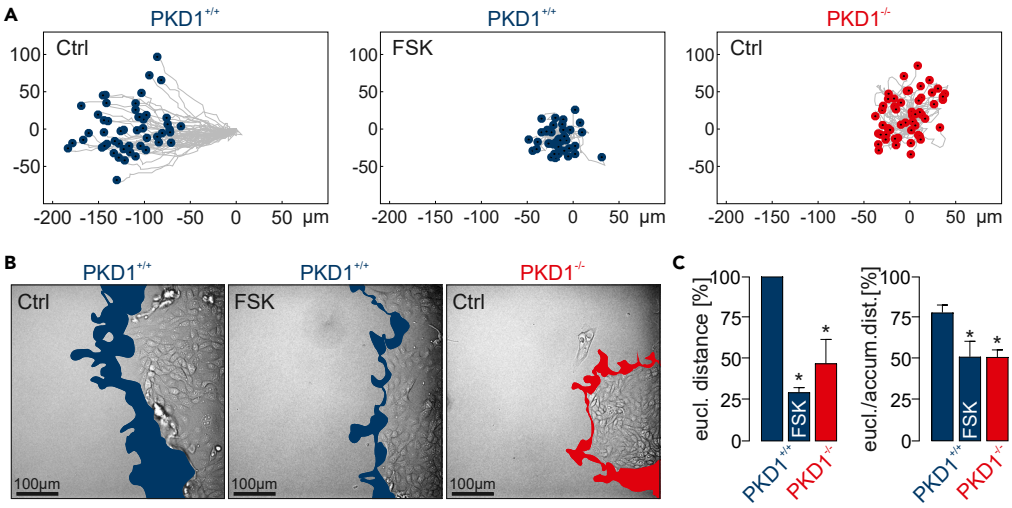

Figure 2. Lack of PC1 along with increase of cAMP leads to defective cell migration

(A) Tracks of individual cells (50 cells per condition from n = 3 individual experiments) imaged for 6 h in wound healing assays starting 2 h after wounding the cell monolayer. Deletion of PC1 ($PKD1^{-/-}$; red) resulted in reduced migration. The same was obtained when incubating PC1-competent cells ($PKD1^{+/+}$; blue) with forskolin.

(B) Representative images of wound healing assays showing the invaded area of cells within 6 h.

(C) Quantification of the euclidean distance of the individually tracked cells (left) and the ratio of euclidean distance in relation to the accumulated distance (right) indicating significant impairment of directed cell migration upon loss of PC1 or application of forskolin in PC1-competent cells. *significant compared to $PKD1^{+/+}$-Ctrl. Data are represented as mean ± SEM. See also Figure S6, Videos S2 and S3.

of prolyl hydroxylation by 2-(1-chloro-4- hydroxyisoquinoline-3-carboxamido) acetate (ICA) which prevents HIF-degradation, HIF-1α inhibition by acriflavin (ACF) or application of ATP have an impact on the formation of cysts or tubular structures in the 3D matrix (Figure S5). In contrast to cAMP, neither ICA, ACF nor ATP exerted considerable influence on the architecture of cell aggregation of PC1-competent cells (forming tubules) or PC1-deficient cells (forming cysts) (Figure S5) excluding a significant impact of HIF or ATP on the morphological differences in our cell clones.

PC1-deficiency and increased cAMP concentration impair motility and directed cell migration of renal tubule cells

Tubule formation including elongation and repair depends on sustained cell motility and directed cell migration (Lienkamp et al., 2012) (and Figure S6 and Video S2). In the 3D matrix experiments we have observed a reduced motility of the cell aggregates upon loss of PC1 or increase of cAMP. Next to the overall motility, we wanted to test for effects on directed cell migration. Therefore, we performed single cell tracking in wound healing assays (Figure 2 and Video S3). PC1-competent cells migrated toward the wound in a directed manner (Figure 2 and Video S3). In contrast, PC1-deficient cells showed significantly reduced directed migration (Figure 2 and Video S3). Application of forskolin significantly diminished directed cell migration in PC1-competent cells comparable to PC1-deficient cells tracked under control condition (Figure 2 and Video S3). Significant reduction of the ratio of euclidean distance compared to accumulated distance illustrates that impairment of cell movement was not solely caused by reduction in overall motility but also by alterations in orientated migration (Figure 2C).

Loss of PC1 leads to cAMP-dependent change in planar cell organization

Since lack of PC1 along with increased levels of cAMP resulted in a switch from tubulogenesis to cystogenesis as well as reduced directed migration, we wanted to test for additional changes in cell orientation. Planar cell polarity (PCP) plays a crucial role for the proper development and maintenance of tubules. Disturbances of PCP may promote tubular dilation and early cyst formation (Lienkamp et al., 2012; Nigro et al., 2015). Therefore, we next monitored colony formation of outgrowing single clonal cells to identify genotype-phenotype related correlations (Figure 3). Colonies of PC1-competent cells were characterized by a scattered appearance of individual cells with rather irregular colony borders interrupted by numerous

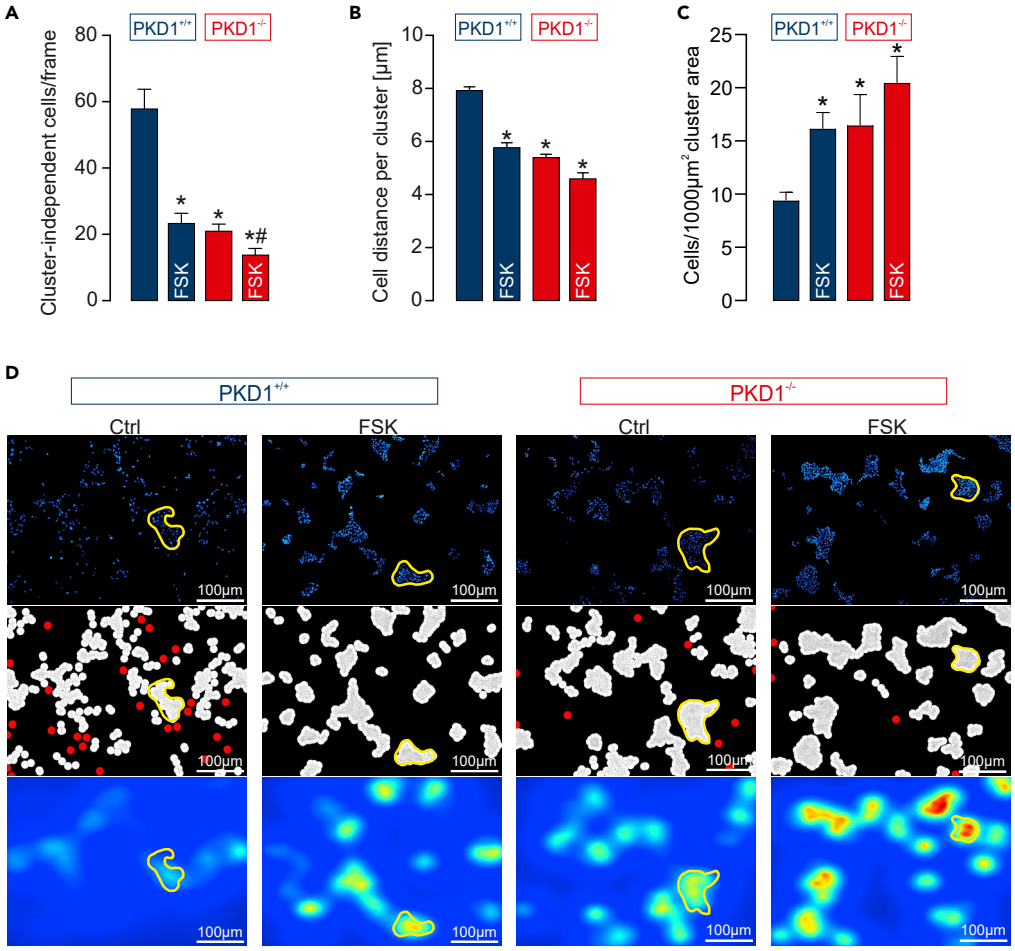

Figure 3. Loss of PC1 and increase of cAMP lead to dense cell aggregation and reduction of disseminating single cells

PC1-competent cells ($PKD1^{+/+}$) and PC1-deleted cells ($PKD1^{-/-}$) were cultured at low density (3200 cells/cm^2) and analyzed with regard to their growing pattern.

(A) PC1-competent cells kept growing in a disseminated pattern forming small colonies with a significant amount of single cluster-independent cells. PC1-deleted cells resulted in dense and evenly bordered cell aggregations with only a few single cells being detectable outside these cell formations. Forskolin (FSK; 10µM) significantly reduced the number of single PC1-competent and PC1-deficient cells (analysis of 72 images from n = 3 individual experiments).

(B) Voronoi-based analysis of cell distance between clustering cells (defined as > two cells). Cell distance was significantly higher in PC1-competent cells compared to PC1-deficient cells and PC1-competent cells in the presence of forskolin.

(C) Analysis of cell density within bigger cell aggregates (comprising 10 - 50 cells/cluster). Cells were significantly less dense within the clusters of PC1-competent cells under control condition compared to PC1-deficient cells or PC1-competent cells in the presence of forskolin.

(D) Representative images after 48 h of culture of PC1-competent cells ($PKD1^{+/+}$) and PC1-deficient cells ($PKD1^{-/-}$) under control condition (Ctrl) or in the presence of forskolin (FSK; 10µM). Row 1 shows representative images of DAPI-stained cells. In each image, one cell cluster was marked by a yellow outline in order to facilitate finding of the corresponding parts in the Voroni-based animations and heat map analyses. Row 2 shows Voronoi-based animation of cell clusters (defined as > two cells; white) and single cells (red). Row 3 shows heatmap analysis of cells visualizing cell density defined as blue = low cell density and red = high cell density. *significant compared to $PKD1^{+/+}$-Ctrl. # significant compared to $PKD1^{-/-}$-Ctrl. Data are represented as mean ± SEM. See also Figures S7 and S8.

outgrowing and migrating cells (Figures 3A and 3D). In contrast, PC1-deficient cells revealed a more compact cell organization with a more defined colony border and only few migrating cells (Figures 3A and 3D). In addition, when comparing cell clustering (defined as more than two cells) by unbiased Voronoi interpolations, cell distance was significantly higher in PC1-competent cells under control condition than in PC1-deficient cells and PC1-competent cells in the presence of forskolin (Figures 3B and 3D). Furthermore,

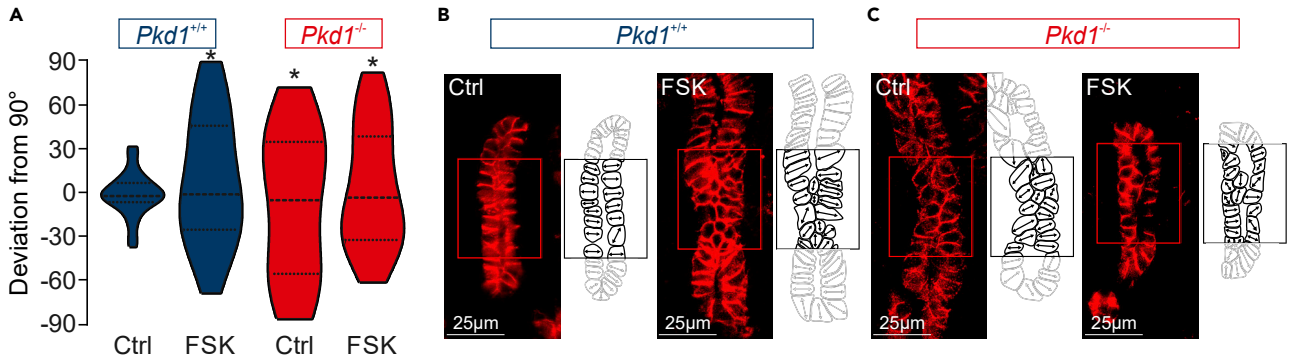

Figure 4. PC1 deletion and cAMP increase lead to impaired epithelial tubular cell orientation in metanephric mouse kidneys

Metanephric kidneys (n = 3 per condition) from KspCreER^{T2}:*Pkd1*$^{lox;lox}$ mice were dissected at embryonic day 13.5 and either incubated with control medium in order to preserve PC1 expression (*Pkd1*$^{+/+}$) or medium supplemented with hydroxytamoxifen (500 nM) resulting in tubule-specific deletion of PC1 (*Pkd1*$^{-/-}$). Thereafter, kidneys were cultured *ex vivo* for five days either incubated with control medium (Ctrl) or in the presence of forskolin (FSK; 10µM). (A) Violin plots illustrating the deviation of the tubule cell's longitudinal axis from the longitudinal tubular axis with a reference angle set = 90° (n = 30 tubules per condition with a mean of 10 analyzed cells per tubule).

(B and C) Representative images of metanephric kidneys stained for E-Cadherin illustrating tubule epithelial cell borders and binarized images with depicted longitudinal cell axes. *significant compared to PKD1$^{+/+}$-Ctrl. Data are represented as mean ± SEM.

when analyzing cell density in bigger cell aggregates (defined as at least 10 cells) visualized by heat map analyses, PC1-competent cells were significantly less dense compared to PC1-deficient cells and PC1-competent cells stimulated with forskolin (Figures 3C and 3D). Similar results were obtained by the use of the cAMP and cGMP phosphodiesterase inhibitor IBMX in PC1-competent cells (Figure S7). Collectively, altered colony morphology and cluster organization indicated changes in planar cell orientation by loss of PC1. Application of forskolin or IBMX to PC1-competent cells induced a cluster organization with reduced cell surface area, better defined colony borders and less outgrowing cells highly resembling PC1-deficient cells under control condition.

Additionally, we analyzed cluster organization in PC1-competent and PC1-deficient plMDCK monolayers upon application of the prolyl-hydroxylase inhibitor ICA, HIF-inhibitor ACF, ATP, and the ATP scavenger apyrase. None of these substances affected plMDCK cell organization (Figure S8).

In summary, these findings suggest that increase of cAMP upon loss of PC1 may result in altered cluster formation and organization due to defects in planar cell orientation.

PC1 deficiency along with elevated cAMP results in defective orientation of tubular cells in developing mouse kidneys

Our previous findings indicated that PC1 deficiency resulted in impaired tubulogenesis and cell orientation in a cAMP-dependent manner *in vitro*. Next, we analyzed metanephric mouse kidneys for defects in tubular cell arrangement and tubule formation. Interestingly, tubule-specific knockout of Pkd1 as well as application of forskolin induced cyst formation in *ex vivo* cultured metanephric mouse kidneys (Kraus et al., 2016b). We harvested metanephric kidneys from inducible tubule-specific Pkd1 knockout mice at embryonic day 13.5 and cultured them *ex vivo*. Pkd1 knockout was induced by application of hydroxy-tamoxifen as described previously (Kraus et al., 2016b). Both, PC1-competent as well as PC1-deficient kidneys were either incubated with forskolin or kept under control conditions for five days. Then, kidney sections were stained for E-Cadherin to analyze the pattern of planar cell arrangement within the renal (non-cystic) tubules. Longitudinal orientation of E-cadherin positive tubular cells was nearly parallel in non-induced PC1-competent kidneys (Figure 4). In contrast, mediolateral orientation was significantly altered in PC1-deficient kidneys (Figure 4) which was in line with previous findings (Castelli et al., 2013). Application of forskolin in control kidneys resulted in reduced mediolateral orientation of E-Cadherin positive tubular cells highly resembling PC1-deficient kidneys (Figure 4). Forskolin in addition to PC1 deletion led to similar distributions of tubular cells deviating from their designated orientation along the tubular axis compared to PC1-deleted kidneys incubated with control medium. However, cystic phenotype differed between these two conditions as PC1-deficient kidneys co-stimulated with forskolin had significantly higher cystic indices as shown previously (Magenheimer et al., 2006; Schreiber et al., 2019). If worsening of the cystic

phenotype by forskolin could exclusively be explained by chloride secretion-mediated cyst enlargement of already formed cysts or if additive cAMP increase in PC1-deficient tubule cells further perturbed tubule development remained unclear. However, this issue may be addressed *in vitro*. We therefore wondered if PC1-competent and PC1-deficient cysts in the presence of forskolin can be stimulated to form tubules and if so, if the phenotype differed depending on the genotype.

Capacity for tubule formation upon increase of cAMP is more reduced in PC1-deficient cells than in PC1-competent cells

Hepatocyte growth factor (HGF) causes MDCK cysts to produce branching tubules within several days (Zegers et al., 2003). In line with these findings, HGF tended to increase the number of tubule-like structures in PC1-competent cells in the presence of control medium (Figure S9). However, HGF showed no impact on PC1-competent cysts in the presence of forskolin as well as PC1-deficient cysts in the presence or absence of forskolin (Figure S9). We next wondered if there was a stronger stimulus that could overcome cAMP-mediated cyst growth and lead to tubule formation. Kidney injury induces gene expression of tubule epithelial cells that significantly overlaps with expression profile found during metanephric kidney development (Kirita et al., 2020). Therefore, we wanted to test if injury of the cyst-lining epithelium can cause repair by forming tubular structures. To achieve this, we established a novel technique through which injury was induced by puncture of cysts within a collagen I matrix with a pulled glass capillary microneedle and the use of a micromanipulator (Figure 5, Videos S4 and S5). As shown before, PC1-competent cells formed cysts within a collagen matrix in the presence of forskolin (Figure 5). Needle-induced injury of the cyst mediated cellular repair by growing out a tubule. However, this was only obtained in 35.9 $\pm$ 5.9% of injured PC1-competent cysts indicating impaired capacity of tubule formation in the presence of forskolin (Figure 5). Injury of PC1-deleted cysts of comparable sizes only resulted in tubulogenesis in 16.0 $\pm$ 6.4% of cases (Figure 5). Furthermore, the small number of tubules that formed in PC1-deficient cysts were smaller and grew much slower (Figures 5B and 5C). These data further indicate that increase of cAMP impairs tubule formation of renal tubule cells but also show that exogenously induced increase of cAMP in PC1-deleted cells reduces the capacity of tubule formation to a greater extent than in PC1-competent cells.

DISCUSSION

Loss of PC1 is a common prerequisite of cyst formation in ADPKD (Harris and Torres, 2009). However, the downstream effectors leading to cystogenesis are largely unknown. The second messenger cAMP is increased in cystic kidneys and its contribution to ADPKD pathophysiology has therefore been intensively studied (Sussman et al., 2020). cAMP is synthesized by adenylyl cyclases from ATP. It functions as a second messenger to transfer signals from G-protein ligands subsequently resulting in activation of protein kinases, ion channels or induction of gene expression (Sussman et al., 2020). In ADPKD, cAMP has mainly been characterized as a mediator of cyst enlargement by activation of cAMP-induced chloride secretion (Terryn et al., 2011). cAMP is induced by arginine vasopressin (AVP) in ADPKD patients by stimulation of vasopressin 2 receptors (V2R) that are expressed in the basolateral membrane of cyst-lining cells (Meijer et al., 2011; Torres et al., 2012). Next to the exogenous stimulation, additional endogenous pathways have been discussed to result in cAMP elevation upon loss of PC1. For instance, reduction of intracellular calcium levels may affect cAMP synthesis owing to activation of calcium-inhibitable adenylyl cyclases 5 and 6 (Rees et al., 2014; Wang et al., 2018). In addition, inhibition of calcium-calmodulin-dependent PDE1 may reduce cAMP hydrolysis (Sussman et al., 2014). The underlying mechanisms resulting in elevated levels of cytosolic cAMP in ADPKD cyst-lining cells are still not clear. Our findings support the idea that deletion of PC1 leads to endogenous induction of cAMP independent from extracellular stimuli since cAMP measurements in our experiments were performed in serum-free medium. However, we cannot rule out that cAMP may be additionally elevated by extracellular stimuli in experiments using serum-containing medium and that PC1-deficient cells may be more susceptible to hormones such as AVP that stimulate Gs-coupled receptors.

Increased concentration of cAMP following PC1 deletion was accompanied by a significant decrease in tubule epithelial cell migration, alterations in planar cell organization and mis-orientation of cells along the tubule system in embryonic kidneys. MDCK cells are widely used to study polarization, migration and cyst formation. As described, we used pIMDCK cells, a subclone that expresses PC1 at detectable protein levels. The presence of PC1 may explain why our control cells form tubule-like structures within a collagen I matrix under control conditions whereas other reports described cyst formation using MDCK cells under similar conditions and the need for overexpression approaches in order to study PC1 function (Boca et al.,

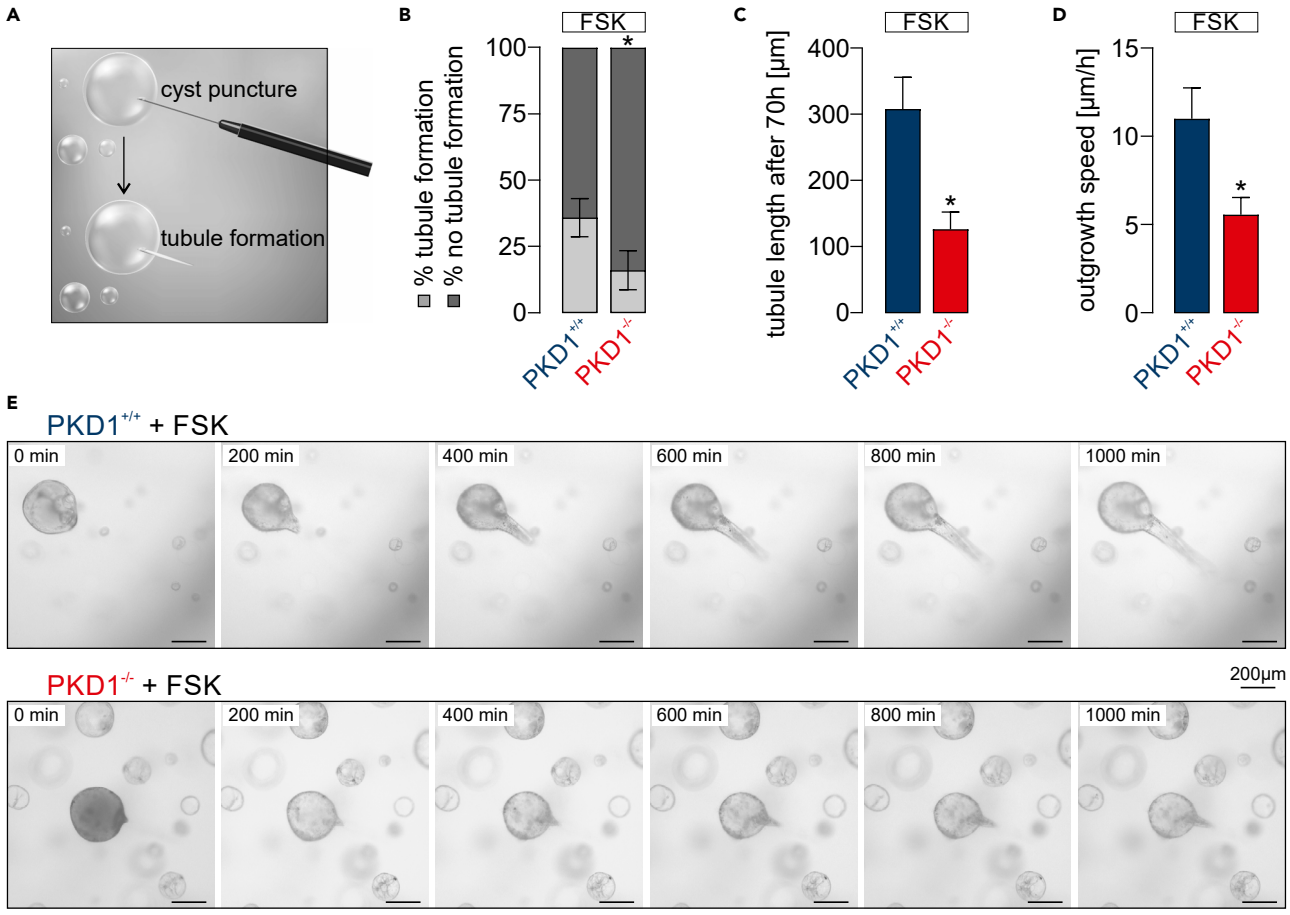

Figure 5. cAMP leads to impaired capacity for tubule formation but is more pronounced in PC1-deficient cells

PC1-competent ($PKD1^{+/+}$) and PC1-deficient cells ($PKD1^{-/-}$) were cultured within a collagen matrix in the presence of forskolin (FSK; 10µM) where they formed cysts within four days. Thereafter PC1-competent cysts (n = 47 from three individual experiments) and PC1-deficient cysts (n = 75 from four individual experiments) were punctured with a pulled glass capillary microneedle and the use of a micromanipulator. Punctured cysts were imaged for 70 h as depicted in (A).

(B) Analysis of the ratio of cysts forming tubules after injury.

(C) Analysis of the length of the formed tubules within 70 h.

(D) Outgrowth speed of the formed tubules by tracking the distance within 1000 min (measured from minute 100 to 1100 after injury).

(E) Representative images showing tubular outgrowth in PC1-competent and PC1-deficient cysts. *significant compared $PKD1^{+/+}$. Data are represented as mean ± SEM. See also Figure S9, Videos S4 and S5.

2007; Boletta et al., 2000). However, in line with our findings, overexpression of PC1 in MDCK cells resulted in a gain of tubulogenesis, whereas control clones (which did not express PC1) formed cysts (Boletta et al., 2000). Similarly, a switch from tubule to cyst formation has been described in epithelial *Pkd1* knockout cells derived from $Pkd1^{flox/-}$ mice (Merrick et al., 2012).

Cyst formation is associated with the induction of numerous signaling pathways. A very robust finding is the activation of ERBB receptor tyrosine kinases (EGFR/ERBB1, HER2/ERBB2, ERBB3, and ERBB4) that induce multiple signaling cascades comprising RAF, MEK1/2, and ERK1/2 kinases (Seeger-Nukpezah et al., 2015). In the kidney, ERBB proteins are involved in tubulogenesis and are essential for renal development by controlling proliferation and orientation, in particular, polarization of tubule epithelial cells (Kee et al., 1997; Veikkolainen et al., 2012). Upstream of ERBB, the cytoplasmic tyrosine kinase SRC mediates phosphorylation of EGFR in the catalytic domain which stabilizes kinase activation and promotes activation of RAF-kinases (Biscardi et al., 1999; Parker et al., 2020). Furthermore, SRC enhances EGFR-dependent activation of the JAK-STAT pathway further promoting cyst growth (Silva, 2004; Strubl et al., 2020). Interestingly, SRC has been shown to be activated by cAMP-induced protein kinase A (Wang and Zhuang, 2017). Therefore,

it is intriguing to speculate, that endogenous elevation of cAMP upon loss of PC1 may be an early event in cyst initiation, subsequently leading to activation of signaling cascades comprising ERBB, RAF, ERK, JAK-STAT, altogether contributing to cyst formation. In addition, cyst growth may further be promoted by exogenous stimulation of Gs-coupled receptors as shown for AVP binding to V2R (Torres et al., 2012).

Tubule-specific deletion of Pkd1 in metanephric mouse kidneys resulted in cyst formation and was accompanied by a significant increase of mis-orientated cells along the developing tubular system. To our surprise, pharmacological elevation of cAMP by forskolin in Pkd1-competent kidneys resulted in a very similar phenotype. Cyst formation in metanephric kidneys has primarily been attributed to induction of cAMP-induced chloride secretion leading to tubular dilations owing to a lack of efflux as developing nephrons and collecting ducts have not yet connected (Buchholz et al., 2014b; Magenheimer et al., 2006). However, recently it has been shown that antagonists of EGFR and SRC inhibited forskolin-dependent cyst formation in Pkd1-metanephric mouse kidneys (Jansson et al., 2012). This strengthens the hypothesis that increase of cAMP may be an early event initiating cyst formation by activation of SRC- and ERBB- mediated signaling pathways.

Our data suggest a threshold for cytoplasmic cAMP that needs to be reached to induce cellular alterations resulting in defective migration and causing a switch from tubulogenesis to cyst formation. Loss of PC1 results in critical increase of cAMP. This assumption is based on the finding that loss of PC1 resulted in comparable phenotypes that were obtained from PC1-competent cells incubated with forskolin although reaching higher cAMP concentrations. In addition, no significant additive effects on cyst formation, directed cell migration, and cell cluster assembly were obtained when applying forskolin to PC1-deficient cells. In the metanephric kidneys, forskolin, PC1 deletion as well as the combination of both resulted in similarly altered distributions of tubular cells deviating from their designated orientation along the tubular axis. However, cyst growth was increased in PC1-deficient kidneys if co-stimulated with forskolin as shown previously (Magenheimer et al., 2006; Schreiber et al., 2019). We assumed that cyst growth in the PC1-deficient metanephric organs was primarily mediated by cAMP-dependent activation of apical chloride secretion. However, we could not rule out additive cyst initiation events by further increase of cAMP. The data obtained from our novel injury-induced tubule formation model suggested that forskolin resulting in comparable levels of cAMP in PC1-competent and PC1-deficient cells had a stronger effect on suppressing tubule outgrowth in PC1-deficient cells. This may be caused by additional but cAMP-independent effects. Alternatively, cAMP may promote stronger activation of downstream signaling pathways in cells lacking PC1 compared to PC1-competent cells. It would be interesting to address this question in future studies.

Next to our findings obtained from tubule epithelial cells, PC1-deficient lymphatic endothelial cells also showed defective directed migration as well as PC1-deficient mouse embryo fibroblasts (Boca et al., 2007; Outeda et al., 2014). It would be intriguing to see if these alterations may also result from changes in cAMP levels and therefore represent a general cellular mechanism caused by loss of PC1 or if our findings are specific for renal tubule cells.

In conclusion, this study emphasizes the importance of cAMP in ADPKD whose increase upon loss of PC1 significantly may trigger the initiation of renal cyst formation. Therefore, cAMP may not only qualify as a target to inhibit cyst enlargement but also to prevent initiation of cyst formation.

Limitations of the study

Our study has several limitations: 1) experiments were conducted with MDCK cells and embryonic mouse kidneys. Therefore, in future studies it would be interesting to analyze human cells and tissue. 2) The mechanism of how loss of PC1 leads to increase in cAMP is not clear. 3) Ideally, we would have been able to lower cAMP in PC1-deficient cells to test if this reverses the phenotypic changes that we find upon loss of PC1. However, due to a lack of reasonable pharmacological strategies, we were not able to address this question.

STAR★METHODS

Detailed methods are provided in the online version of this paper and include the following:

- KEY RESOURCES TABLE
- RESOURCE AVAILABILITY

SUPPLEMENTAL INFORMATION

Supplemental information can be found online at https://doi.org/10.1016/j.isci.2022.104359.

ACKNOWLEDGMENTS

We thank Barbara Teschemacher, Andrea Lüdke and Eugenia Schefler for their excellent technical support. We thank Anselm Hochschild for his help with the python software to edit the heatmaps. BB and JS were supported by the Deutsche Forschungsgemeinschaft (DFG, German Research Foundation), project number 387509280, SFB 1350, projects A2, B3 and C5, respectively). JKS and AK were supported by the Interdisciplinary Center for Clinical Research Erlangen (thesis scholar ship and junior project J71, respectively). This work was performed by JKS and KS in fulfillment of the requirements for obtaining the degree Dr. med and Dr. rer. nat., respectively.

AUTHOR CONTRIBUTIONS

JKS and BB have designed studies, conducted experiments, acquired and analyzed data, and have written the manuscript. AK and KS have conducted experiments, acquired and analyzed data. SG, JS and MS have designed studies and analyzed data. DL has written the software programs.

DECLARATION OF INTERESTS

The authors declare no competing interests.

Received: January 24, 2022
Revised: March 23, 2022
Accepted: April 29, 2022
Published: June 17, 2022

REFERENCES

Biscardi, J.S., Maa, M.C., Tice, D.A., Cox, M.E., Leu, T.H., and Parsons, S.J. (1999). c-Src-mediated phosphorylation of the epidermal growth factor receptor on Tyr845 and Tyr1101 is associated with modulation of receptor function. J. Biol. Chem. *274*, 8335–8343. https://doi.org/10.1074/jbc.274.12.8335.

Boca, M., D'Amato, L., Distefano, G., Polishchuk, R.S., Germino, G.G., and Boletta, A. (2007). Polycystin-1 induces cell migration by regulating phosphatidylinositol 3-kinase-dependent cytoskeletal rearrangements and GSK3β-dependent cell–cell mechanical adhesion. Mol. Biol. Cell *18*, 4050–4061. https://doi.org/10.1091/mbc.e07-02-0142.

Boletta, A., Qian, F., Onuchic, L.F., Bhunia, A.K., Phakdeekitcharoen, B., Hanaoka, K., Guggino, W., Monaco, L., and Germino, G.G. (2000). Polycystin-1, the gene product of PKD1, induces resistance to apoptosis and spontaneous tubulogenesis in MDCK cells. Mol. Cell *6*, 1267–1273. https://doi.org/10.1016/s1097-2765(00)00123-4.

Buchholz, B., Teschemacher, B., Schley, G., Schillers, H., and Eckardt, K.U. (2011). Formation of cysts by principal-like MDCK cells depends on the synergy of cAMP- and ATP-mediated fluid secretion. J. Mol. Med. Berl *89*, 251–261. https://doi.org/10.1007/s00109-010-0715-1.

Buchholz, B., Schley, G., Faria, D., Kroening, S., Willam, C., Schreiber, R., Klanke, B., Burzlaff, N., Jantsch, J., Kunzelmann, K., and Eckardt, K.U. (2014a). Hypoxia-inducible factor-1αCauses renal cyst expansion through calcium-activated chloride secretion. J. Am. Soc. Nephrol. *25*, 465–474. https://doi.org/10.1681/asn.2013030209.

Buchholz, B., Faria, D., Schley, G., Schreiber, R., Eckardt, K.U., and Kunzelmann, K. (2014b). Anoctamin 1 induces calcium-activated chloride secretion and proliferation of renal cyst-forming epithelial cells. Kidney Int. *85*, 1058–1067. https://doi.org/10.1038/ki.2013.418.

Cabrita, I., Kraus, A., Scholz, J.K., Skoczynski, K., Schreiber, R., Kunzelmann, K., and Buchholz, B. (2020). Cyst growth in ADPKD is prevented by pharmacological and genetic inhibition of TMEM16A *in vivo*. Nat. Commun. *11*, 4320. https://doi.org/10.1038/s41467-020-18104-5.

Castelli, M., Boca, M., Chiaravalli, M., Ramalingam, H., Rowe, I., Distefano, G., Carroll, T., and Boletta, A. (2013). Polycystin-1 binds Par3/aPKC and controls convergent extension during renal tubular morphogenesis. Nat. Commun. *4*, 2658. https://doi.org/10.1038/ncomms3658.

Chebib, F.T., and Torres, V.E. (2016). Autosomal dominant polycystic kidney disease: core curriculum 2016. Am. J. Kidney Dis. Off. J. Natl. Kidney Found. *67*, 792–810. https://doi.org/10.1053/j.ajkd.2015.07.037.

Chebib, F.T., Sussman, C.R., Wang, X., Harris, P.C., and Torres, V.E. (2015). Vasopressin and disruption of calcium signalling in polycystic kidney disease. Nat. Rev. Nephrol. *11*, 451–464. https://doi.org/10.1038/nrneph.2015.39.

Chebib, F.T., Perrone, R.D., Chapman, A.B., Dahl, N.K., Harris, P.C., Mrug, M., Mustafa, R.A., Rastogi, A., Watnick, T., Yu, A.S.L., and Torres, V.E. (2018). A practical guide for treatment of rapidly progressive ADPKD with tolvaptan. J. Am. Soc. Nephrol. *29*, 2458–2470. https://doi.org/10.1681/asn.2018060590.

Cornec-Le Gall, E., Audrezet, M.P., Le Meur, Y., Chen, J.M., and Ferec, C. (2014). Genetics and pathogenesis of autosomal dominant polycystic kidney disease: 20 years on. Hum. Mutat. *35*, 1393–1406. https://doi.org/10.1002/humu.22708.

Gattone, V.H., Wang, X., Harris, P.C., and Torres, V.E. (2003). Inhibition of renal cystic disease development and progression by a vasopressin V2 receptor antagonist. Nat. Med. *9*, 1323–1326. https://doi.org/10.1038/nm935.

Gekle, M., Wünsch, S., Oberleithner, H., and Silbernagl, S. (1994). Characterization of two MDCK-cell subtypes as a model system to study principal cell and intercalated cell properties. Pflügers Arch. Eur. J. Physiol. *428*, 157–162. https://doi.org/10.1007/bf00374853.

Grantham, J.J., Mulamalla, S., and Swenson-Fields, K.I. (2011). Why kidneys fail in autosomal dominant polycystic kidney disease. Nat. Rev. Nephrol. *7*, 556–566. https://doi.org/10.1038/nrneph.2011.109.

Harris, P.C., and Torres, V.E. (2009). Polycystic kidney disease. Annu. Rev. Med. *60*, 321–337. https://doi.org/10.1146/annurev.med.60.101707.125712.

Hildebrandt, F., Benzing, T., and Katsanis, N. (2011). Ciliopathies. N. Engl. J. Med. *364*, 1533–1543. https://doi.org/10.1056/nejmra1010172.

Jansson, K., Nguyen, A.N.T., Magenheimer, B.S., Reif, G.A., Aramadhaka, L.R., Bello-Reuss, E., Wallace, D.P., Calvet, J.P., and Blanco, G. (2012). Endogenous concentrations of ouabain act as a cofactor to stimulate fluid secretion and cyst growth of *in vitro* ADPKD models via cAMP and EGFR-Src-MEK pathways. Am. J. Physiol. Ren. Physiol. *303*, F982–F990. https://doi.org/10.1152/ajprenal.00677.2011.

Kee, N., McTavish, A.J., Papillon, J., and Cybulsky, A.V. (1997). Receptor protein tyrosine kinases in perinatal developing rat kidney. Kidney Int. *52*, 309–317. https://doi.org/10.1038/ki.1997.336.

Kirita, Y., Wu, H., Uchimura, K., Wilson, P.C., and Humphreys, B.D. (2020). Cell profiling of mouse acute kidney injury reveals conserved cellular responses to injury. Proc. Natl. Acad. Sci. *117*, 15874–15883. https://doi.org/10.1073/pnas.2005477117.

Kraus, A., Grampp, S., Goppelt-Struebe, M., Schreiber, R., Kunzelmann, K., Peters, D.J., Leipziger, J., Schley, G., Schodel, J., Eckardt, K.U., and Buchholz, B. (2016a). P2Y2R is a direct target of HIF-1α and mediates secretion-dependent cyst growth of renal cyst-forming epithelial cells. Purinergic Signal *12*, 687–695. https://doi.org/10.1007/s11302-016-9532-5.

Kraus, A., Schley, G., Kunzelmann, K., Schreiber, R., Peters, D.J.M., Stadler, R., Eckardt, K.U., and Buchholz, B. (2016b). Glucose promotes secretion-dependent renal cyst growth. J. Mol. Med. Berl *94*, 107–117. https://doi.org/10.1007/s00109-015-1337-4.

Kraus, A., Peters, D.J.M., Klanke, B., Weidemann, A., Willam, C., Schley, G., Kunzelmann, K., Eckardt, K.-U., and Buchholz, B. (2018). HIF-1α promotes cyst progression in a mouse model of autosomal dominant polycystic kidney disease. Kidney Int. *94*, 887–899. https://doi.org/10.1016/j.kint.2018.06.008.

Lantinga-van Leeuwen, I.S., Leonhard, W.N., van der Wal, A., Breuning, M.H., de Heer, E., and Peters, D.J. (2007). Kidney-specific inactivation of the Pkd1 gene induces rapid cyst formation in developing kidneys and a slow onset of disease in adult mice. Hum. Mol. Genet. *16*, 3188–3196. https://doi.org/10.1093/hmg/ddm299.

Lienkamp, S.S., Liu, K., Karner, C.M., Carroll, T.J., Ronneberger, O., Wallingford, J.B., and Walz, G. (2012). Vertebrate kidney tubules elongate using a planar cell polarity-dependent, rosette-based mechanism of convergent extension. Nat. Genet. *44*, 1382–1387. https://doi.org/10.1038/ng.2452.

Magenheimer, B.S., St John, P.L., Isom, K.S., Abrahamson, D.R., De Lisle, R.C., Wallace, D.P., Maser, R.L., Grantham, J.J., and Calvet, J.P. (2006). Early embryonic renal tubules of wild-type and polycystic kidney disease kidneys respond to cAMP stimulation with cystic fibrosis transmembrane conductance regulator/Na(+),K(+),2Cl(-) Co-transporter-dependent cystic dilation. J. Am. Soc. Nephrol. *17*, 3424–3437. https://doi.org/10.1681/asn.2006030295.

Meijer, E., Bakker, S.J.L., van der Jagt, E.J., Navis, G., de Jong, P.E., Struck, J., and Gansevoort, R.T. (2011). Copeptin, a surrogate marker of vasopressin, is associated with disease severity in autosomal dominant polycystic kidney disease. Clin. J. Am. Soc. Nephrol. *6*, 361–368. https://doi.org/10.2215/cjn.04560510.

Merrick, D., Chapin, H., Baggs, J.E., Yu, Z., Somlo, S., Sun, Z., Hogenesch, J.B., and Caplan, M.J. (2012). The γ-secretase cleavage product of polycystin-1 regulates TCF and CHOP-mediated transcriptional activation through a p300-dependent mechanism. Dev. Cell *22*, 197–210. https://doi.org/10.1016/j.devcel.2011.10.028.

Nigro, E.A., Castelli, M., and Boletta, A. (2015). Role of the polycystins in cell migration, polarity, and tissue morphogenesis. Cells *4*, 687–705. https://doi.org/10.3390/cells4040687.

Outeda, P., Huso, D.L., Fisher, S.A., Halushka, M.K., Kim, H., Qian, F., Germino, G.G., and Watnick, T. (2014). Polycystin signaling is required for directed endothelial cell migration and lymphatic development. Cell Rep. *7*, 634–644. https://doi.org/10.1016/j.celrep.2014.03.064.

Parker, M.I., Nikonova, A.S., Sun, D., and Golemis, E.A. (2020). Proliferative signaling by ERBB proteins and RAF/MEK/ERK effectors in polycystic kidney disease. Cell. Signal. *67*, 109497. https://doi.org/10.1016/j.cellsig.2019.109497.

Raphael, K.L., Strait, K.A., Stricklett, P.K., Miller, R.L., Nelson, R.D., Piontek, K.B., Germino, G.G., and Kohan, D.E. (2009). Inactivation of Pkd1 in principle cells causes a more severe cystic kidney disease than in intercalated cells. Kidney Int. *75*, 626–633. https://doi.org/10.1038/ki.2008.659.

Rees, S., Kittikulsuth, W., Roos, K., Strait, K.A., Van Hoek, A., and Kohan, D.E. (2014). Adenylyl cyclase 6 deficiency ameliorates polycystic kidney disease. J. Am. Soc. Nephrol. *25*, 232–237. https://doi.org/10.1681/asn.2013010077.

Schreiber, R., Buchholz, B., Kraus, A., Schley, G., Scholz, J., Ousingsawat, J., and Kunzelmann, K. (2019). Lipid peroxidation drives renal cyst growth *in vitro* through activation of TMEM16A. J. Am. Soc. Nephrol. *30*, 228–242. https://doi.org/10.1681/asn.2018010039.

Seeger-Nukpezah, T., Geynisman, D.M., Nikonova, A.S., Benzing, T., and Golemis, E.A. (2015). The hallmarks of cancer: relevance to the pathogenesis of polycystic kidney disease. Nat. Rev. Nephrol. *11*, 515–534. https://doi.org/10.1038/nrneph.2015.46.

Silva, C.M. (2004). Role of STATs as downstream signal transducers in Src family kinase-mediated tumorigenesis. Oncogene *23*, 8017–8023. https://doi.org/10.1038/sj.onc.1208159.

Smith, C.E.L., Lake, A.V.R., and Johnson, C.A. (2020). Primary cilia, ciliogenesis and the actin cytoskeleton: a little less resorption, A little more actin please. Front. Cell Dev. Biol. *8*, 622822. https://doi.org/10.3389/fcell.2020.622822.

Strubl, S., Torres, J.A., Spindt, A.K., Pellegrini, H., Liebau, M.C., and Weimbs, T. (2020). STAT signaling in polycystic kidney disease. Cell. Signal. *72*, 109639. https://doi.org/10.1016/j.cellsig.2020.109639.

Sussman, C.R., Ward, C.J., Leightner, A.C., Smith, J.L., Agarwal, R., Harris, P.C., and Torres, V.E. (2014). Phosphodiesterase 1A modulates cystogenesis in zebrafish. J. Am. Soc. Nephrol. *25*, 2222–2230. https://doi.org/10.1681/asn.2013040421.

Sussman, C.R., Wang, X., Chebib, F.T., and Torres, V.E. (2020). Modulation of polycystic kidney disease by G-protein coupled receptors and cyclic AMP signaling. Cell. Signal *72*, 109649. https://doi.org/10.1016/j.cellsig.2020.109649.

Terryn, S., Ho, A., Beauwens, R., and Devuyst, O. (2011). Fluid transport and cystogenesis in autosomal dominant polycystic kidney disease. Biochim. Biophys. Acta *1812*, 1314–1321. https://doi.org/10.1016/j.bbadis.2011.01.011.

Torres, V.E. (2004). Cyclic AMP, at the hub of the cystic cycle. Kidney Int. *66*, 1283–1285. https://doi.org/10.1111/j.1523-1755.2004.00945.x.

Torres, V.E., Chapman, A.B., Devuyst, O., Gansevoort, R.T., Grantham, J.J., Higashihara, E., Perrone, R.D., Krasa, H.B., Ouyang, J., Czerwiec, F.S., et al. (2012). Tolvaptan in patients with autosomal dominant polycystic kidney disease. N. Engl. J. Med. *367*, 2407–2418. https://doi.org/10.1056/nejmoa1205511.

Veikkolainen, V., Naillat, F., Railo, A., Chi, L., Manninen, A., Hohenstein, P., Hastie, N., Vainio, S., and Elenius, K. (2012). ErbB4 modulates tubular cell polarity and lumen diameter during kidney development. J. Am. Soc. Nephrol. JASN *23*, 112–122. https://doi.org/10.1681/asn.2011020160.

Wang, J., and Zhuang, S. (2017). Src family kinases in chronic kidney disease. Am. J. Physiol. Ren. Physiol. *313*, F721–F728. https://doi.org/10.1152/ajprenal.00141.2017.

Wang, Q., Cobo-Stark, P., Patel, V., Somlo, S., Han, P.-L., and Igarashi, P. (2018). Adenylyl cyclase 5 deficiency reduces renal cyclic AMP and cyst growth in an orthologous mouse model of polycystic kidney disease. Kidney Int. *93*, 403–415. https://doi.org/10.1016/j.kint.2017.08.005.

Ye, H., Wang, X., Sussman, C.R., Hopp, K., Irazabal, M.V., Bakeberg, J.L., LaRiviere, W.B., Manganiello, V.C., Vorhees, C.V., Zhao, H., et al. (2016). Modulation of polycystic kidney disease severity by phosphodiesterase 1 and 3 subfamilies. J. Am. Soc. Nephrol. *27*, 1312–1320. https://doi.org/10.1681/asn.2015010057.

Zegers, M.M.P., O'Brien, L.E., Apos Brien, L.E., Yu, W., Datta, A., and Mostov, K.E. (2003). Epithelial polarity and tubulogenesis *in vitro*. Trends Cell Biol. *13*, 169–176. https://doi.org/10.1016/s0962-8924(03)00036-9.

STAR★METHODS

KEY RESOURCES TABLE

REAGENT or RESOURCE	SOURCE	IDENTIFIER
Antibodies		
primary PC1 antibody	Santa Cruz Biotechnology, TX, USA	7e12; RRID: AB_2163355
DAPI	Sigma-Aldrich, Taufkirchen, Germany	D9542
Chemicals, peptides, and recombinant proteins		
SpCas9(BB)-2A-puro-vector (PX459) V2.0	Addgene, Watertown, MA, USA	ID 62988
pGL3 Luciferase Reporter Vector	Promega, Madison, WI, USA	E1751
ECL Femto Substrate	ThermoFisher, Waltham, MA, USA	34094
2-(1-chloro-4- hydroxyisoquinoline-3-carboxamido) acetate (ICA)	Gift from Prof. Nicolai Burzlaff, Dpt. of Chemistry and Pharmacy, University Erlangen-Nuernberg, Germany	
Forskolin	Sigma-Aldrich	F6886
ATP	Sigma-Aldrich	A6419
Acriflavine	Sigma-Aldrich	A8126
DMSO	Carl Roth	A994.1
(Z)-4-hydroxytamoxifen	Sigma-Aldrich	H7904
PureCol®, Bovine Collagen	CellSystems, Troisdorf, Germany	5005
brilliant cresyl blue	Carl Roth, Karlsruhe, Germany	5162.1
Critical commercial assays		
cAMP-Screen Direct System	Applied Biosystems, Foster City, CA, USA	P/N 4412186
Experimental models: Cell lines		
principal-like Madin-Darby Canine Kidney cells (plMDCK cells) subclone	Gekle et al., 1994, Buchholz et al., 2011	
Experimental models: Organisms/strains		
KspCreER^{T2}:*Pkd1*$^{lox;lox}$ (tamoxifen-inducible, kidney epithelium-specific Pkd1-deletion mouse model)	Gift from Prof. Dorien J.M. Peters (Dpt. of Human Genetics, Leiden University, Netherlands)	Lantinga-van Leeuwen et al., 2007
Oligonucleotides		
Guide primers Exon 1 fw 5′-CACCGTGCTCCGGGCATTGGACGTT Exon 1 rev 5′-AAACAACGTCCAATGCCCGGAGCAC	Sigma-Aldrich	
Cloning primers Exon 1 clon fw 5′-GCATGGTACCCAGAAAGGGAA TGGCGCAG Exon 1 clon rev 5′-GCTAGCTAGCGCTTGGCTAAT GACACCCAC	Sigma-Aldrich	
Off-target primers Chrom 34 fw 5′-ACGTAAGCGGCAAGAGTCAA Chrom 34 rev 5′-CTGCCTTCATCACTCCCAGG Chrom 3 fw 5′-AATTGGCTGCTGTGCAAAGC Chrom 3 rev 5′-CAGCCTCTCCCCATAGCAAG	Sigma-Aldrich	
Software and algorithms		
Guide RNA design algorithm	Zhang laboratory, Cambridge, MA, USA	http:/crispr.mit.edu/

(*Continued on next page*)

Continued

REAGENT or RESOURCE	SOURCE	IDENTIFIER
ImageJ	ImageJ Version 1.52a	National Institute of Health, RRID:SCR_003070 (https://imagej.nih.gov/ij/)
Fiji Morphological Segmentation Plugin	MorphoLibJ	https://imagej.net/plugins/morpholibj
Chemotaxis and Migration Tool Software	ibidi, Graefelfing, Germany	https://ibidi.com/chemotaxis-analysis/171-chemotaxis-and-migration-tool.html
gnuplot software (Graphs visualization)	gnuplot	http://www.gnuplot.info
Matplotlib (Jupyterlab Version 3.2.9)	Matplotlib	https://matplotlib.org/
Python software	Python	www.python.org
Other		
Sanger Sequencing	eurofins, Nuernberg, Germany	
glass capillaries	World Precision Instruments, Friedberg, Germany	1.14 mm 3.5″; 504949
Micropipette puller	World Precision Instruments	PUL-1000; WPI
MicroGrinder	Narishige, Tokyo	EG-401
Micro injector	World Precision Instruments	SMARTouch MICO02T
Organotypic cell culture inserts, Millicell 0,4μM, 30mm	Merck Millipore	PICM03050

RESOURCE AVAILABILITY

Lead contact

Further information and requests for resources and reagents should be directed to and will be fulfilled by the lead contact, Bjoern Buchholz (bjoern.buchholz@uk-erlangen.de).

Materials availability

This study did not generate new unique reagents.

Data and code availability

All data reported in this paper will be shared by the lead contact upon request. This paper does not report original code. Any additional information required to reanalyse the data reported in this paper is available from the lead contact, Bjoern Buchholz (bjoern.buchholz@uk-erlangen.de), upon request.

EXPERIMENTAL MODEL AND SUBJECT DETAILS

plMDCK cell culture

plMDCK cell clone was subcloned from the American Type Culture Collection (ATCC, Rockville, Md., USA; catalogue no. CCL 34) MDCK cells, which originate from a healthy female cocker spaniel, and were obtained at passage 62 (Buchholz et al., 2011). plMDCK cells were cultured up to passage 82 at 37°C, 21% O_2 and 5% CO_2 in Dulbecco's modified eagle medium supplemented with 2 mM L-glutamine, 10% heat-inactivated fetal calf serum, 50U/L penicillin and 50U/l streptomycine.

Pkd1 mouse model

Animal experiments were approved by the local institutional review board and all animal experiments complied with the with the United Kingdom Animals Act, 1986, and associated guidelines, EU Directive 2010/63/EU for animal experiments. Experiments were approved by the local Ethics Committee of the Government of Unterfranken/Wuerzburg (AZ: RUF 55.2.2-2532.2-853-13). Generation of mice with a tamoxifen-inducible, kidney epithelium-specific Pkd1-deletion (KspCreER^{T2}:*Pkd1*$^{lox;lox}$) was described recently (Lantinga-van Leeuwen et al., 2007). Mice were a kind gift from Prof. Dorien J.M. Peters (Department of Human Genetics, Leiden University Medical Center, Leiden, The Netherlands) and were crossed back into a C57BL/6 background as described previously (Cabrita et al., 2020). Animals were hosted on a 12:12 h light:dark cycle under constant temperature (24 ± 1 °C) in standard cages. They were fed a standard diet with free access to tap water.

METHOD DETAILS

Generation of PC1-deficient plMDCK cells

Guide RNAs targeting Exon 2 of the Pkd1 gene were ligated with a pSpCas9(BB)-2A-puro-vector (PX459) V2.0 from Addgene (ID 62988; Watertown, MA, USA). Guide RNA design was performed based on an algorithm provided by the Zhang laboratory (http:/crispr.mit.edu/) (Figure S1). Then, 10^6 principal-like MDCK-cells (passage 80-82) were transfected with 10μL polyethylenimine and 4 μg DNA and were subsequently seeded in 3.5 cm dishes. After incubation with puromycine (3.5 μg/mL), single cell clones were generated by dilution. Genomic DNA of these single cell clones was isolated and the target region of the guide RNA was amplified by PCR. For mutation screens, the following PCR products were analyzed by polyacrylamide gel electrophoresis (PAGE). For analysis of clones of cells with putative indel mutations, PCR products were cloned into a pGL3 vector (Promega, Madison, WI, USA) and analyzed via Sanger Sequencing (eurofins, Nuernberg, Germany). Generated clones were then used at passages 7-15.

cAMP measurements

plMDCK cells were grown in a pre-coated assay capture plate (cAMP-Screen Direct System P/N 4412186; Applied Biosystems, Foster City, CA, USA) in serum-free medium. Cells were exposed to serum-free control medium or control medium supplemented with 10μM forskolin. cAMP measurements were performed by the use of the GloMax-Multi Detection System (Promega, Fitchburg, Madison, USA) according to the manufacturer's protocol.

Immunoblotting

0.7×10^6 cells were seeded within a 10 cm dish. After three days, medium was changed and 24 h later, cells were resuspended and pelleted by centrifugation at 2500 rpm for 3 min. The supernatant was discarded and pellets were resuspended in lysis buffer (25 mM Tris-HCl, 150 mM NaCl, 100 mM dithiothreitol, 5.5% Nonident P-40, 5% glycerol, 1 mM EDTA, 1% protease inhibitor (cOmplete, Roche, Mannheim). After sonification and centrifugation (14,000 g for 20 min at 4°C), samples were separated within a 3–8% Tris-acetate gel. Gels underwent dry transfer onto a PVDF membrane. Membranes then were blocked by TBS supplemented with 5% nonfat dry milk and 0.1% Tween 20 (TBS-T). Incubation with primary PC1 antibodies (7e12, Santa Cruz) was performed overnight at 4°C and was followed by incubation with horseradish peroxidase-conjugated secondary antibody. The membranes were visualized via ECL Femto Substrate (ThermoFisher, Waltham, Massachusetts, USA) with Amersham Imager.

Cell migration assays

Cells were seeded in 2-well cell culture inserts on μ-Slides 4-well (ibidi, Graefelfing, Germany). After 24 h, cells were serum starved overnight and treated with or without forskolin (10μM). Time-lapse microscopy was started 2 h after wounding. Every 5 min, seven microscope fields per well at a magnification of x20 were taken for 6 h. Images were taken with a BZ-9000 microscope with an incubation chamber (Keyence, Osaka, Japan). For analyzing cell motility, movement of the cell nuclei was followed by using the manual-tracking plugin from ImageJ. Cell paths were analyzed using the Chemotaxis and Migration Tool Software (ibidi): Accumulated distance = $\sum$(distance(T_{n+1}-T_n)); n = 0; 70; Euclidean distance = distance$_{T70}$ – distance$_{T0}$. Graphs were visualized using gnuplot software (http://www.gnuplot.info).

Cell polarity assays

Cells were seeded at low density with or without addition of 10μM forskolin (FSK), 100μM ATP, 100 nM acriflavine (ACF) (all Sigma-Aldrich, Taufkirchen, Germany) or 10μM prolyl hydroxylation 2-(1-chloro-4- hydroxyisoquinoline-3-carboxamido) acetate (ICA) (kind gift from Prof. Nicolai Burzlaff, Department of Chemistry and Pharmacy, University Erlangen-Nuernberg, Germany) and incubated for 48 h. Then, cells were fixated with paraformaldehyde (4%) and stained with DAPI (1:1000) for 1 h at 23 °C. Images were taken using an Olympus IX70 microscope. Then, cell nuclei stained by DAPI were transferred into a coordinate system by the use of ImageJ and the use of "Find Maxima" and "Center of mass". Subsequently, image analyses were performed in Java. Therefore, each coordinate of the image was assigned to the closest cell nucleus center (= Voronoi interpolation) by "tD_max". Then, Voronoi interpolation was extended by restricting components to a maximum distance "d_max" from the center, defined as 17 μm, which is a common length of MDCK cells. Finally, adjacent Voronoi combs were merged to a cluster. Heatmaps of cell centers were generated by Python software (www.python.org/). Since the substances were dissolved in different concentrations of dimethyl sulfoxide (DMSO), we tested for DMSO-dependent effects on cell arrangement and cluster formation in PC1-competent and PC1-deficient cells. No DMSO-dependent effects were observed (Figure S10).

In vitro cystogenesis/ tubulogenesis model

plMDCK cells were resuspended in type I collagen, plated in 24-well plates and incubated at 37°C for 1 h as described previously. Then, medium supplemented with or without 10μM forskolin, 100μM ATP, 10μM ICA or 100 nM ACF was added and changed every 48 h. Images of four random visual fields per well were taken in a blinded manner at ×4 magnification using a Zeiss Primo Vert microscope and a Zeiss Axiocam 105 camera (Zeiss Microscopy GmbH, Jena, Germany) at day five.

Automated segmentation and measurements of *in vitro* cysts and tubules

Segmentation of all structures within the collagen matrix was performed by the use of use of Fiji Morphological Segmentation Plugin of MorphoLibJ (https://imagej.net/plugins/morpholibj). Then, cyst area was set in ratio with tubular area. Cysts were regarded as spherical shaped bodies. Therefore, perimeter of depicted cysts was measured and cyst volume was calculated based on perimeter = $2\pi r$ and volume = $4/3\pi r^3$.

Micromanipulation of *in vitro* cysts

plMDCK cells were grown in type I collagen matrix in the presence of 10μM forskolin to form cysts within four days. Then, micropuncture was performed by the use of glass capillaries (1.14 mm 3.5''; World Precision Instruments) which were pulled with a Micropipette puller (PUL-1000; WPI) and sharpened by the use of a MicroGrinder EG-401 (Narishige, Tokyo, Japan). Then, glass capillaries were loaded with brilliant cresyl blue (50 mg/mL PBS; Roth 5162.1) and puncture was performed with the help of a WPI SMARTouch MICO02T microinjector and a Leica S9D Stereo microscope. 1 nL of the blue dye was injected in every cyst in order to locate them for live imaging. Live images were captured by a BZ-9000 microscope with an incubation chamber (Keyence). N = 47 punctured PC1-competent cysts from three individual experiments and n = 75 punctured PC1-deficient cysts from four individual experiments were monitored for 70 h by capturing images every 20 min.

3D live imaging of spheroid movement

plMDCK spheroids were cultured for four days. Then, images were taken using a BZ-9000 microscope (Keyence) every 60 min for a period of 48 h. For each condition, 10 spheroids were analyzed. Automated image analysis was performed by Python Software. Image pre-processing included equalize_adapthist, unsharp_mask, enhance_contrast, diameter_closing and remove_small_objects modules, Raster scanning of the pre-processed images was performed to detect spheroid outlines. Their visualization and potential blinded manual post-processing included the use of the poly-editor provided by the matplotlib library (https://matplotlib.org).

Metanephric kidney model

Metanephric kidneys were dissected from KspCreER^{T2}:*Pkd1*$^{lox;lox}$ mice at embryonic day 13.5 and cultured on transparent organotypic cell culture inserts (Merck Millipore, PICM03050, Billerica, MA) with or without addition of (Z)-4-hydroxytamoxifen (500 nM, H7904, Sigma-Aldrich) for five days as described previously (Kraus et al., 2016b). Male and female kidneys were used in the experiments. No sex-related differences were noticeable. After 24 h, medium was changed and supplemented with or without 10 μM forskolin. Then, medium was changed again 48 h later. Kidneys were fixated in 4% paraformaldehyde. Thereafter, three kidneys per condition were stained for E-Cadherin and a total of 30 tubules per condition with a mean of 10 cells per tubule were analyzed according to their angular deviation in relation to the longitudinal tubular axis determined by ImageJ. Therefore, the angle between the longest axis of each cell obtained by determination of the maximum diameter and the longitudinal axis of the tubule were calculated in a blinded manner using ImageJ software. An angle of 90° was used as reference which was the typical finding in control and untreated renal tubules. For statistical analysis, number of deviation of angles $\leq 15°$ were compared with the number of deviations >15° and analyzed by the use of Fisher exact test.

QUANTIFICATION AND STATISTICAL ANALYSIS

Data are expressed as mean ± SEM. Differences among groups were analyzed using one-way ANOVA, followed by a Bonferroni test for multiple comparisons. An unpaired *t*-test was applied to compare the differences between two groups. Wilcoxon signed-rank test for columns statistics was used for relative values. Two-sided Fisher's exact test was used to analyze categorical data. $p < 0.05$ was considered statistically significant.